SAND2007-7320C

Distortion of laser-welded thin planar micro-components*

D.O. MacCallum, G.A. Knorovsky, C.V. Robino
Sandia National Laboratories
Albuquerque, NM 87185

2007 AWS Welding Show
Chicago, IL
November 12, 2007

*Sandia is a multiprogram laboratory operated by Sandia Corporation, a Lockheed Martin Company, for the United States Department of Energy's National Nuclear Security Administration under contract DE-AC04-94AL85000.

NNSA National Nuclear Security Administration

Sandia National Laboratories

Residual stresses and distortion result from welding *

Transverse shrinkage

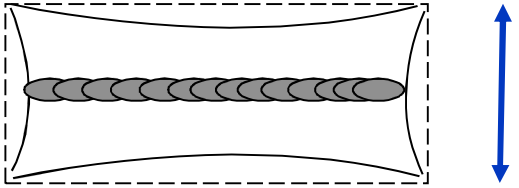

Longitudinal shrinkage

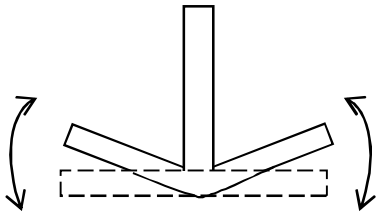

Angular rotations

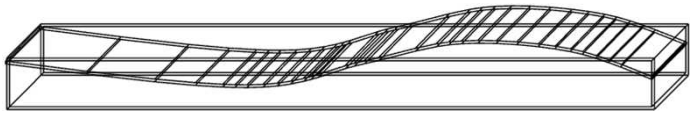

Longitudinal and Buckling distortions

In-plane and out-of-plane distortions

- Weldment is heated locally by the welding heat source; the temperature distribution in the weldment is not uniform in space or time.
- These non-uniform temperature changes cause transient and complex thermal expansion. Non-elastic or incompatible strains are produced in weld and the base metal regions near the weld.
- Transient thermal stresses and long-range metal movements (bending, buckling and rotation) result.
- These displacements are called distortion.
- After welding is completed, residual stresses remain.

**Analysis of Welded Structures, K. Masubuchi*

Sandia National Laboratories

Goal is to show similarities & differences between three regimes of distortion

Macroscopic fusion welding (linear seam) angular distortion: Watanabe-Satoh analytic approach

mm-size laser fusion welding, spot and seam,

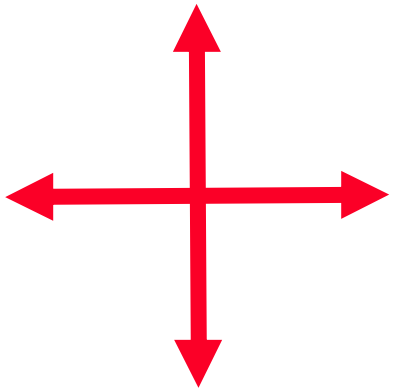

experiment, FEA, modified W-S approach

sub-mm size thermal bending, spot and seam,

experiment, Vollertsen, FEA

Experimental

Melting
~ 1mm thick

Laser spot disc weld (SS)

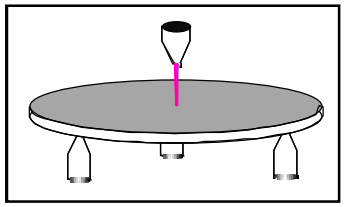

FEM

Unrestrained bend bar, laser seam weld (SS)

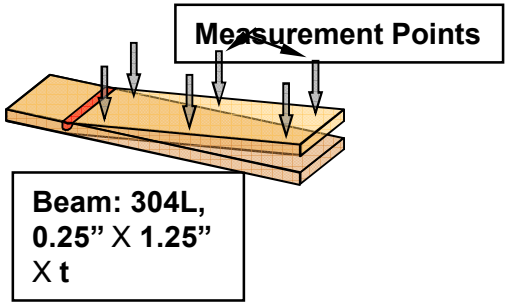

Analytical

Not melting
~ 150 μm thick

Thin bars (NeyoroG Au), discs (SS)

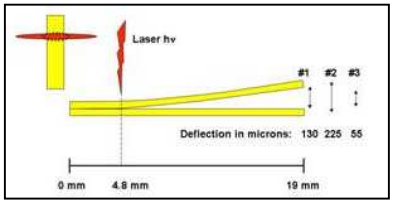

Analytical

&

FEM

Sandia National Laboratories

Distortion Evaluation of 304L SS in Laser Spot Welding

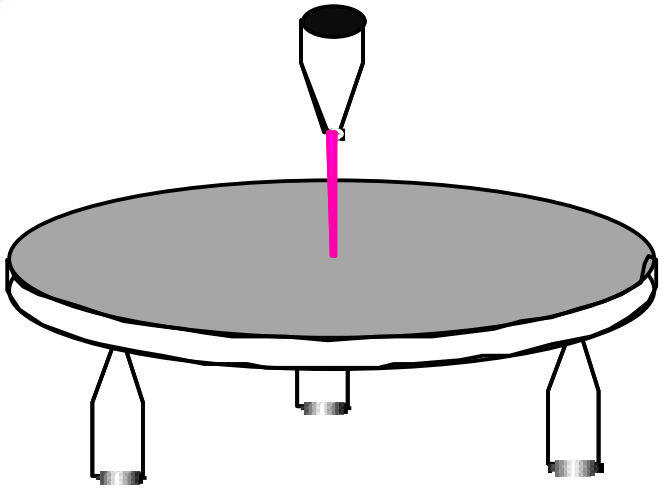

On thin parts, TC attachment can contribute significant residual stresses to the part to be processed.

Estimated effect due to the TC welds is comparable to the non-flatness after lapping.

- Material: 304 Stainless Steel
  - EDM'd from 6.3 mm plate used for calorimetry
- Sample Geometry:
  - 1.2 mm thick,
  - 25.4 mm diameter
  - Flat to within +/- 2 μ
  - Supported on pins to minimize contsraint and conductive loss
- Laser Parameters
  - 1.5 – 5.7 J/p, 2.2 – 7 ms

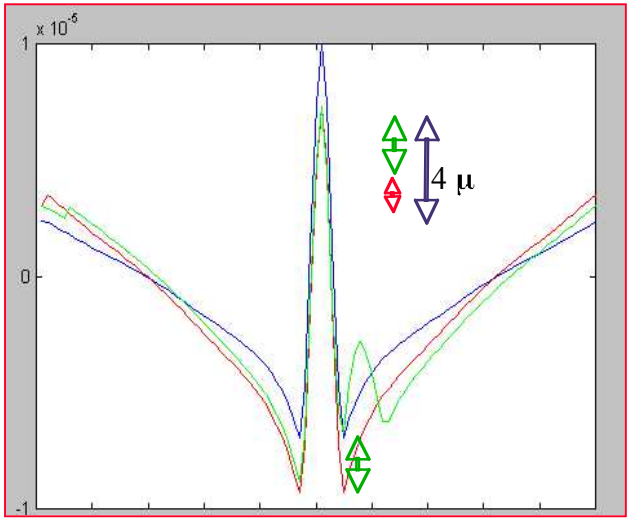

Superimposed distortions of laser spot and 4 TC welds

Sandia National Laboratories

Residual Stresses of a Laser Spot Weld

The residual stress state for 3.33J, 7 ms pulse shows the stress, σ_{xx}, on a x-z plane through the center of the weld.

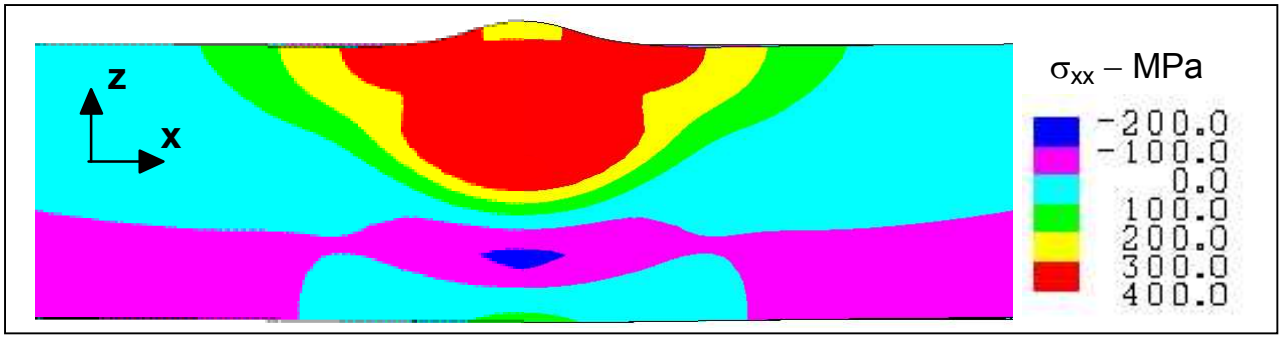

- Stresses are in tension in the fusion zone and nearby material
- Maximum value near 400 MPa.
- A smaller tensile stress exists at the upper surface of the weldment surrounding the fusion zone
- The stress is generally in compression in the lower portion of the disk
- A small region of material is in tension on the bottom of the disk beneath the weld.

Watanabe and Satoh Distortion Evaluation

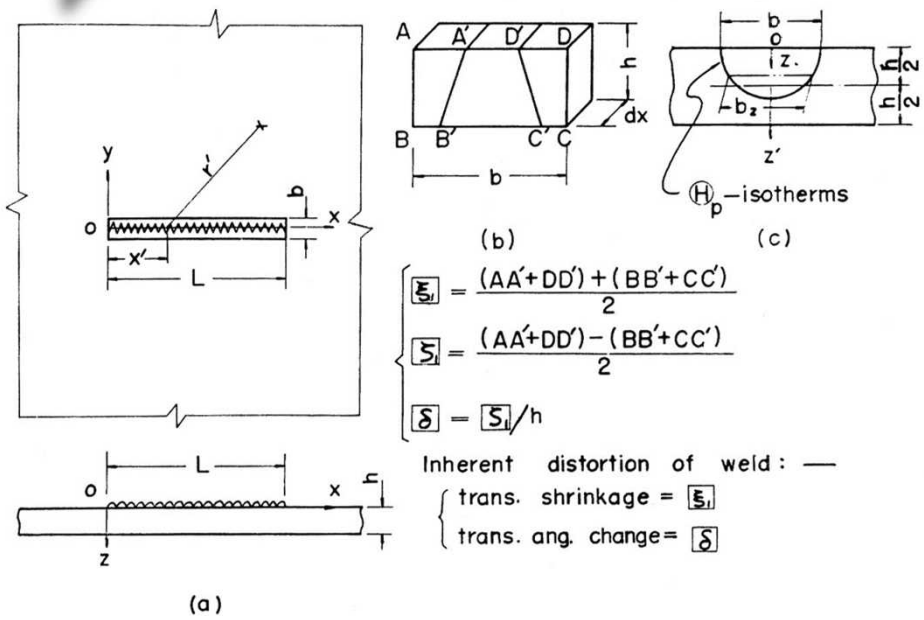

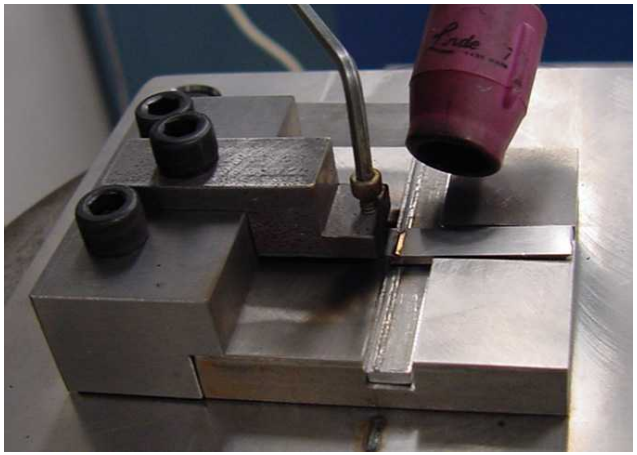

Shield Gas… not arc!

The two distortions of primary interest in the Watanabe and Satoh analysis are transverse shrinkage, ξ, and transverse angular change, δ.

Final distortion is considered to arise from two sources:

- heat input (or temperature gradient) effect
- external restraint (which acts to resist the distortion caused by the former).

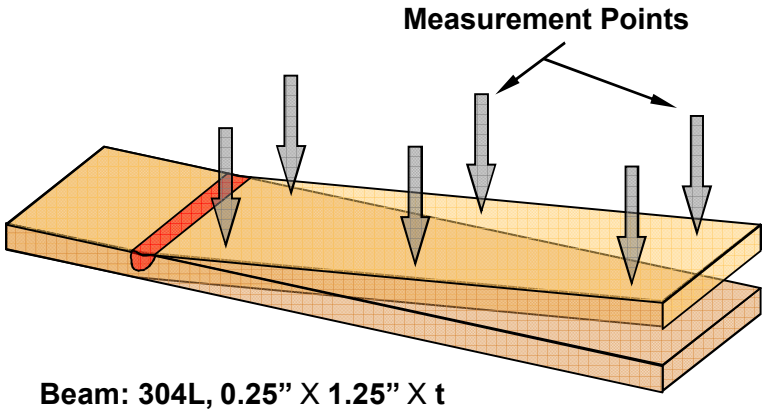

Beam: 304L, 0.25” X 1.25” X t

t ε [0.0.32, 0.045, 0.062]

Key: assess correlations between controllable welding parameters and distortion!

Sandia National Laboratories

Angular Distortions Correlated to Laser Process Factors

Deflection angle vs *process factor*.

$$Angle = f\left(\frac{nQ}{v^{1/2}t^{3/2}}\right)\left(\frac{w}{p}\right)$$

Unrestrained angular distortion in this simple experiment can be correlated over a wide range of laser parameters (and hence weld sizes) by using the Watanabe and Satoh approach

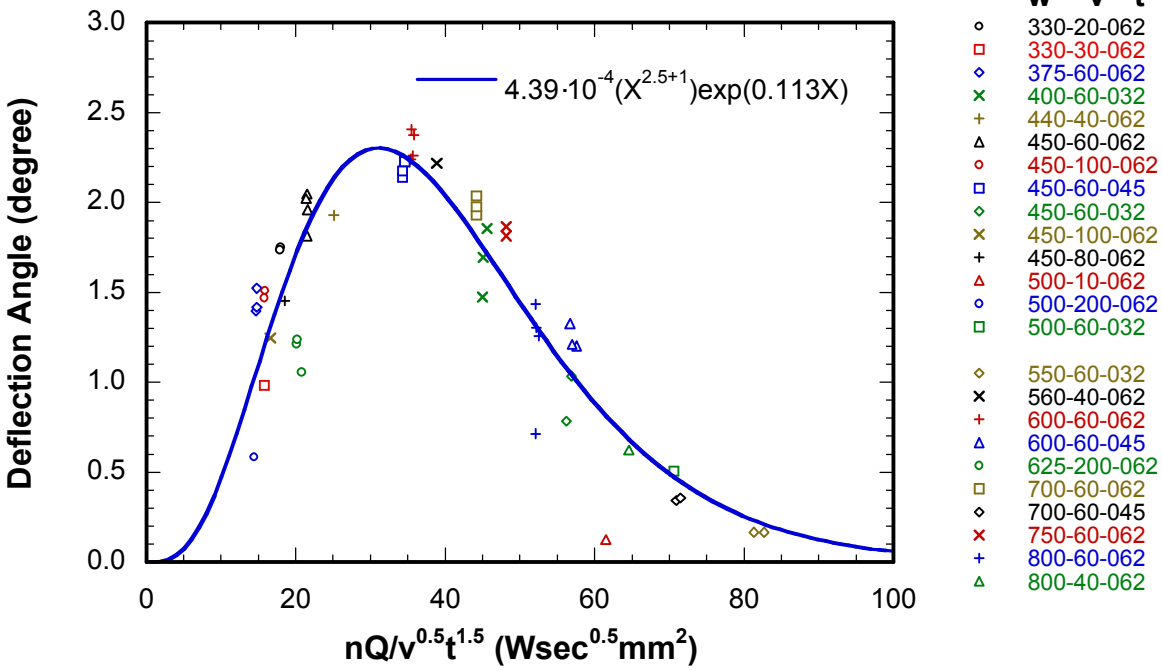

w – v - t

- 330-20-062
- 330-30-062
- 375-60-062
- 400-60-032
- 440-40-062
- 450-60-062
- 450-100-062
- 450-60-045
- 450-60-032
- 450-100-062
- 450-80-062
- 500-10-062
- 500-200-062
- 500-60-032
- 550-60-032
- 560-40-062
- 600-60-062
- 600-60-045
- 625-200-062
- 700-60-062
- 700-60-045
- 750-60-062
- 800-60-062
- 800-40-062

n: energy transfer efficiency

q: delivered power (W)

v: travel speed (mm/sec)

t: thickness in mm.

Sandia National Laboratories

Angular Distortion Correlated to Weld Size

Deflection angle vs *modified thermal process factor*.

$$Angle = \mathbf{f}\left(\frac{nQ}{v^{1/2}t^{3/2}}\right)\left(\frac{w}{p}\right) \xrightarrow[(p = 2A/w)]{(A \propto nQ/v)} Angle = \mathbf{f}\left(\frac{w^2 v^{1/2}}{2t^{3/2}}\right)$$

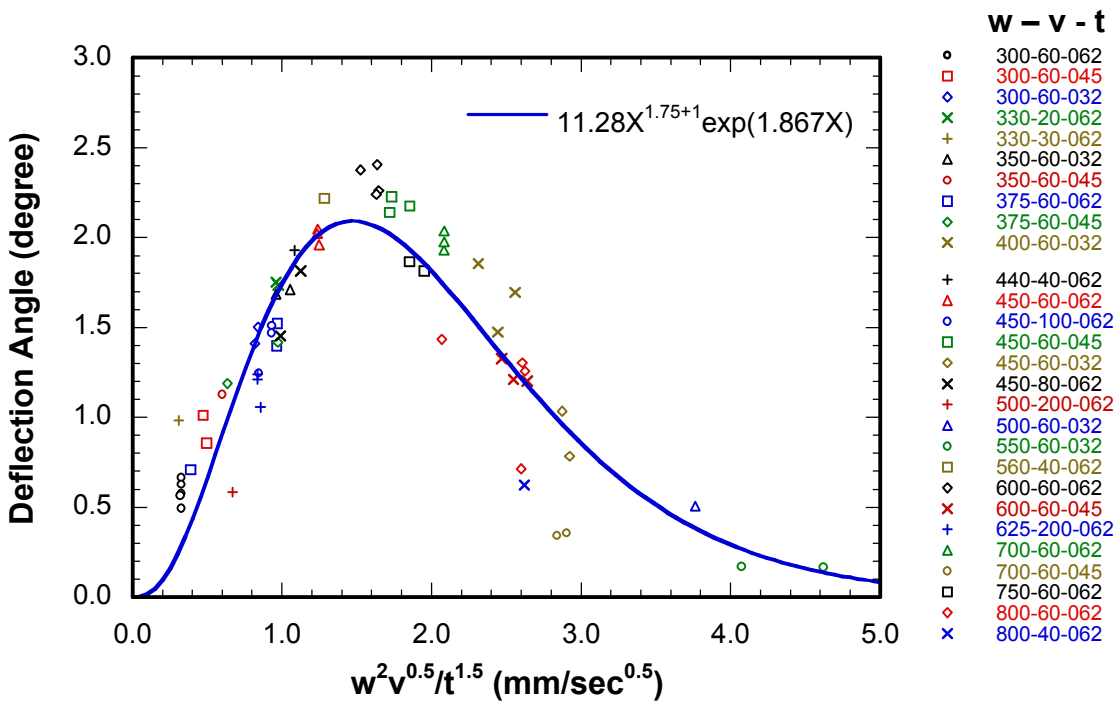

Deflection angle increased with weld width, w, at constant penetration, p.

Angular distortion could also be correlated with a simple function of the weld size.

Sandia National Laboratories

Comparison of W-S with other approaches

TGM $$Angle = \left(\frac{7}{2}\right)\frac{3\alpha_{th}P_1 A}{\rho c_p v S_0^2} - 36\frac{l\sigma_y}{S_0 E}$$

BM $$Angle = \left[36\frac{\alpha_{th}k_f(T_l)}{c_p \rho E}\frac{Ap_l}{\nu_l S_0^2}\right]^{1/3}$$

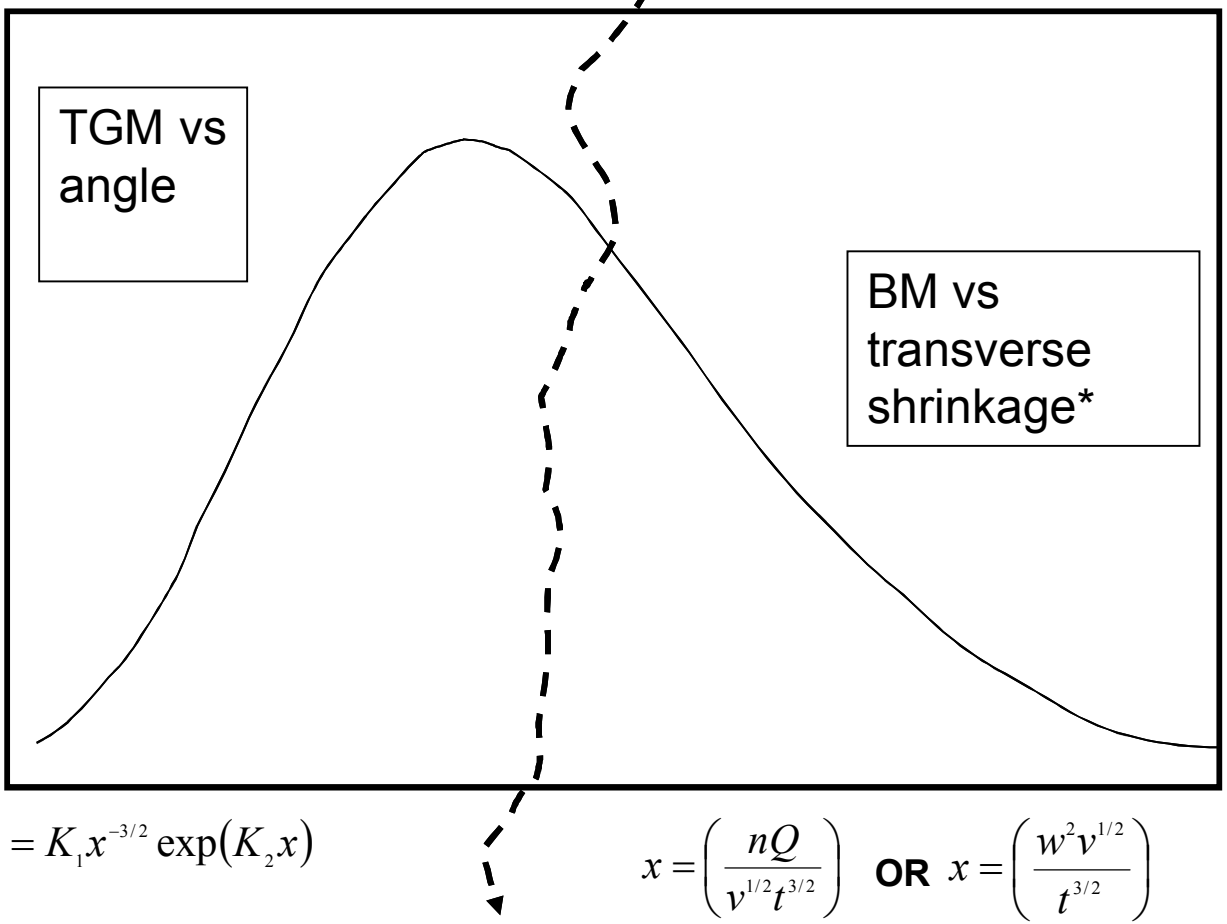

$$Angle = K_1 x^{-3/2}\exp(K_2 x)$$

$$x = \left(\frac{nQ}{v^{1/2}t^{3/2}}\right) \quad \textbf{OR} \quad x = \left(\frac{w^2 v^{1/2}}{t^{3/2}}\right)$$

Sandia National Laboratories

Modeling: analytical

1. Preliminary calculations using analytical expressions developed by Vollertsen, Yau and Magee indicated the possibility of obtaining bending in either Thermal Gradient or Buckling Modes (**TGM** or **BM**).

2. Vollertsen posed a two-layer model for a metal sheet using the TGM. But, a steep transient temperature gradient causes differential thermal strain through the thickness and bending out of plane, initially (on-heating) away from the laser source, then (on-cooling) towards the laser source.

$$\gamma = \left(\frac{7}{2}\right)\frac{3\alpha_{th}P_1A}{\rho c_p \nu S_0^2} - 36\frac{l\sigma_y}{S_0 E}$$

TGM: Yau modified Vollertsen's two-layer TGM development to account for this opposite bend by introducing a second term that takes into account geometric parameters of the sample.

$$\alpha_B = \left[36\frac{\alpha_{th}k_f(T_l)}{c_p\rho E}\frac{Ap_l}{\nu_l S_0^2}\right]^{1/3}$$

BM: Vollertsen's buckling is initiated from uncertain distributions or residual stresses in the material and is applicable for high travel velocities on thin sheets where the thermal conductivity of the material is large compared to the sheet thickness

Sandia National Laboratories

Laser Distortion experiments on cantilever beams of Au-base Neyoro-G™

Bar illumination: a 100mm FL cylindrical lens was used. The focused spot was an elliptical "bar" shaped image (major and minor axes ~15 mm x 0.8 mm, respectively) aimed 4.8 mm from the end of the strip, at a distance of 95 mm from the lens to the part surface.

0.113 mm bending towards beam relative to "flat" part

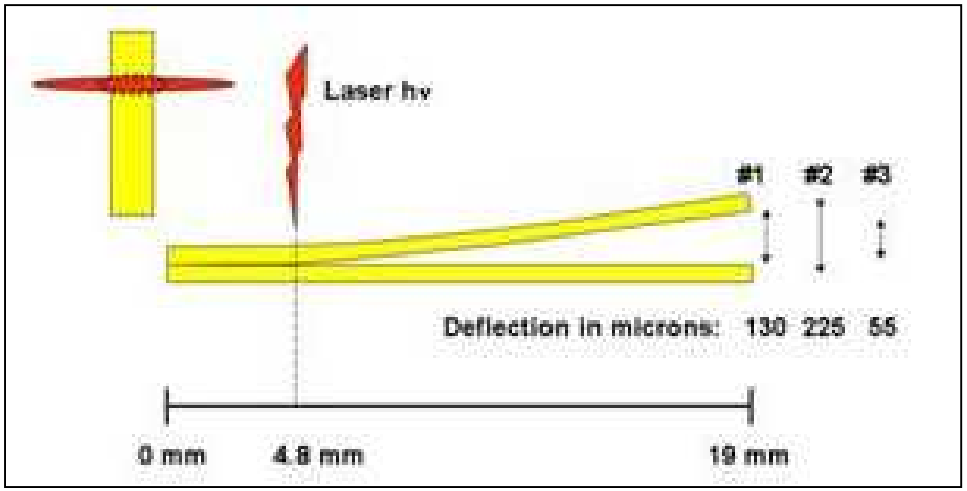

Large deflections

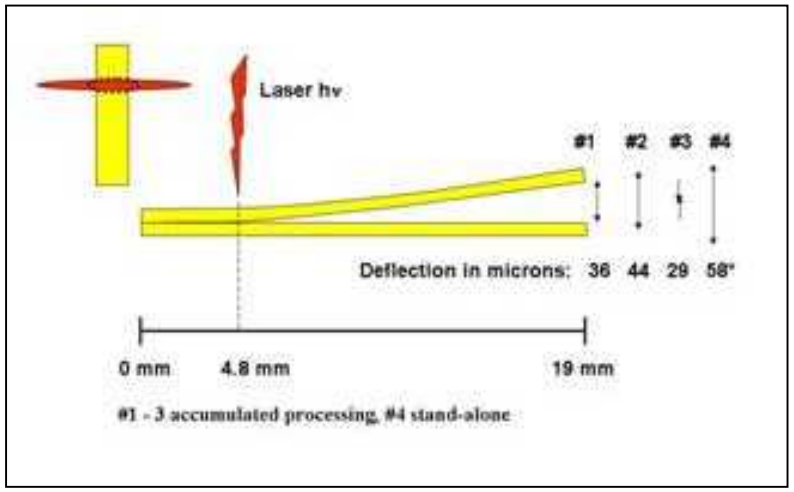

Small deflections

Sandia National Laboratories

Laser Distortion experiments Au-base Neyoro-G™ formed electrical contacts

The measured initial gap showed a large variability: samples 1, 2 and 3 had 336, 689 and 257 μm as-received measured starting gaps, respectively.

- Sample 1 deflected first 21μm, then 10 μm, and finally 17 μm away from the laser beam (closing gap) in sequential runs, decreasing the contact gap a total of 48 μm.
- Sample 2 deflected first 44μm, then 60μm, and finally 9μm away from the laser beam (closing gap) in sequential runs, decreasing the contact gap a total of 113 μm.
- Sample 3 first deflected 22 μm away from the laser beam (closing gap), but on the second run there was no measurable movement observed, and on the third and final run , the contact deflected 20 μm towards the laser beam (opening gap), increasing the contact gap almost the same amount as it decreased during the first run.

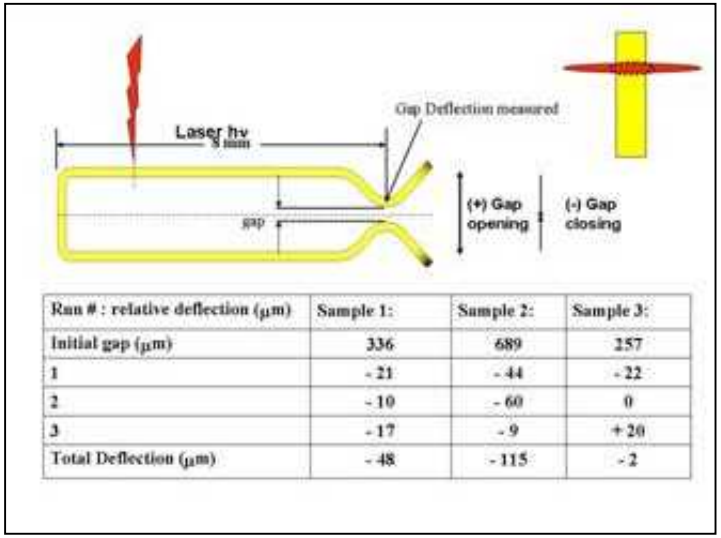

Run # : relative deflection (μm)	Sample 1:	Sample 2:	Sample 3:
Initial gap (μm)	336	689	257
1	- 21	- 44	- 22
2	- 10	- 60	0
3	- 17	- 9	+ 20
Total Deflection (μm)	- 48	- 115	- 2

Contact gap deflections using cylindrical illumination

Sandia National Laboratories

Modeling: the F.E. mesh and boundary conditions

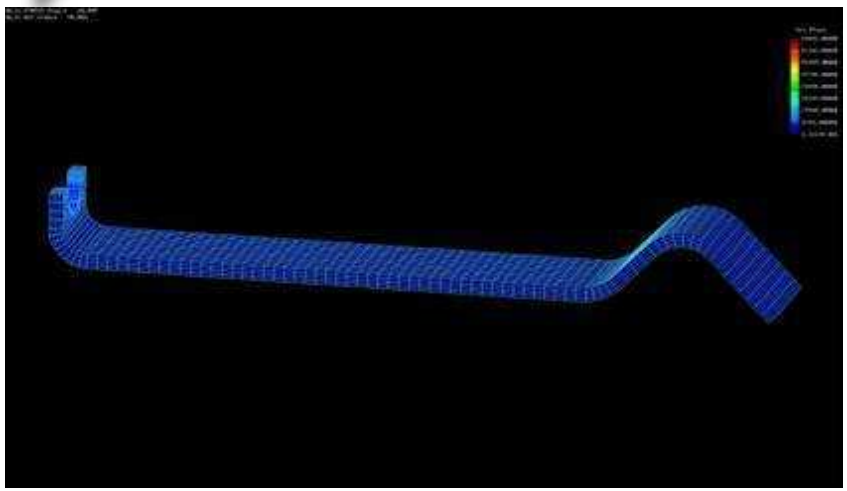

F.E. mesh of contact spring in thermo-mechanical model

- A COSMOS/M® (v2.9) finite element model mesh was used to run a sequential thermal, then mechanical model
- 4275 1st order “Brick” elements; 6364 Nodes
- Thermal calculations included conduction only, no radiative or convective heat flow was assumed
- The boundary conditions at the end (the area where the contact would be riveted to the carrier) were held at the initial temperature, simulating a large heat sink
- A temperature-dependent yield stress was incorporated

- Thermal boundary conditions:
  - uniform initial temp at 72 °F
  - the flat surface and rivet-hole surface held @ 72 °F
  - Heat applied to a surface line at the top surface near the rivet end of the part, either as a bar or translating spot

- Peak volumetric heat flux: $3x10^5$ BTU/in^3-s, with ~4.6W total “bar” heat flux, corresponding to ~3.7kW/mm^2 surface flux.
- The laser source modeled as: a 5 ms turn-on, 2.5 ms hold, 5 ms turn-off heat pulse, (~.01mm spot size)
- For the translating heat source the traverse took 95 ms from initial turn-on to final turn-off (~30 ipm).
- Peak temperature for the translating spot source was 1105 °F and 1338 °F for the bar

Sandia National Laboratories

Modeling: a translating spot on un-restrained parts

Three options were examined:

1) Translating spot simulates a cw weld spot progressing across the surface.

2) Bar-shaped spot simultaneously illuminating an identical width band across the entire contact width.

3) Bar-shaped spot except **with constraint** preventing motion away from the beam-illuminated side during laser illumination.

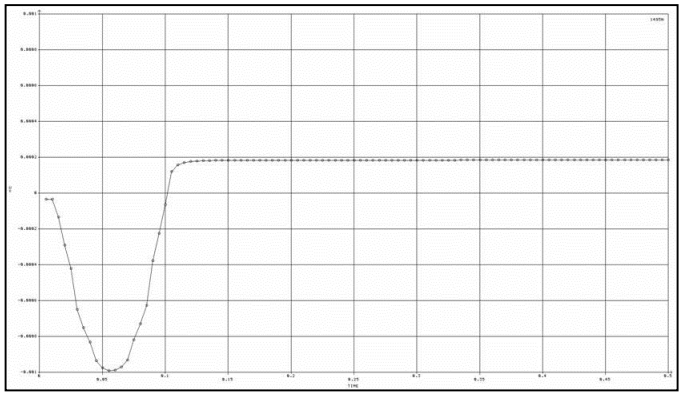

Translating Spot heat source, 10X higher than the bar.

Translating Spot

- The plots follow a node at the extreme right of the contact and tracks its vertical motion.
- For laser conditions which produced an appreciable through-thickness thermal gradient but didn't exceed at the top surface the heat treatment temperature of the Neyoro-G™ (~1000degF), the part:
  - **first bends slightly away from the beam** (on heating)
  - **then does a final bend toward the beam** (on cooling).

Sandia National Laboratories

Modeling: a constant line source on restrained and un-restrained parts

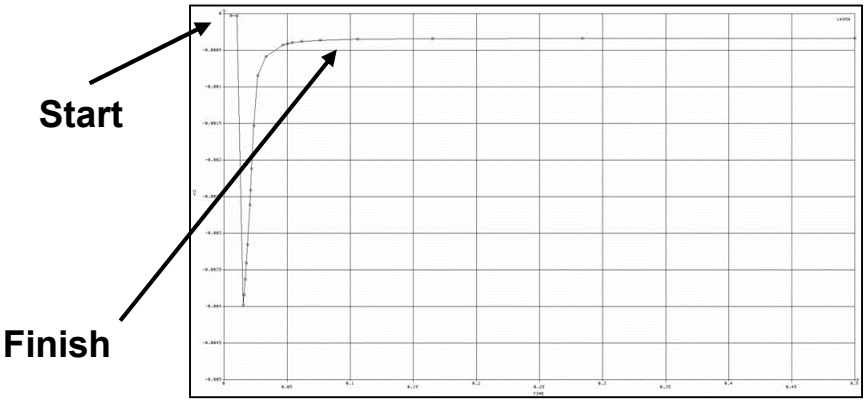

Bar source, not restrained

The laser bar source on the un-restrained contact first causes movement away from the laser source ~ 0.004” but the on-cooling recovery is short of the starting point by about 0.0004”

Final contact gap is 0.0004” larger

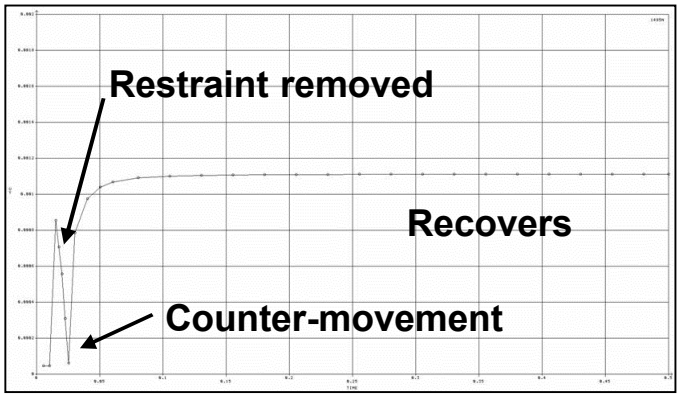

Bar source, restrained. Restraint removed at 0.025 s

The bar source illuminates an initially constrained part. Note that motion is only restrained for the first .025s, after which it is released. Because of the restraint, the tip moves in the opposite sense than when it isn't restrained because the restraint acts like a hinge point. The on-cooling movement is ~ 0.001”

Final contact gap is 0.001” smaller

Sandia National Laboratories

Thermal Measurements and Sample Specifications

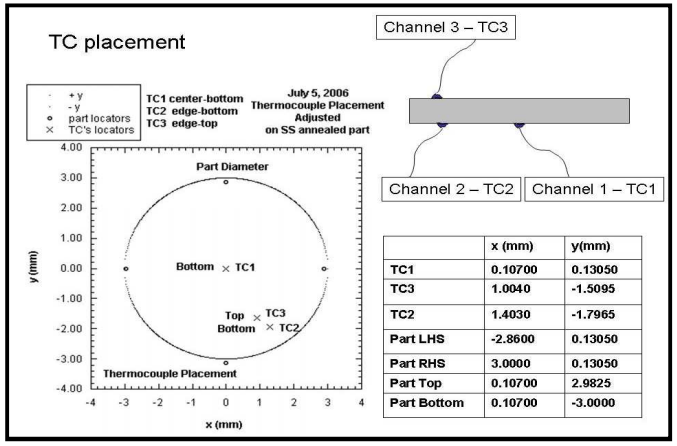

	x (mm)	y(mm)
TC1	0.10700	0.13050
TC3	1.0040	-1.5095
TC2	1.4030	-1.7965
Part LHS	-2.8600	0.13050
Part RHS	3.0000	0.13050
Part Top	0.10700	2.9825
Part Bottom	0.10700	-3.0000

3.5 mm trajectory
on 6 mm part.

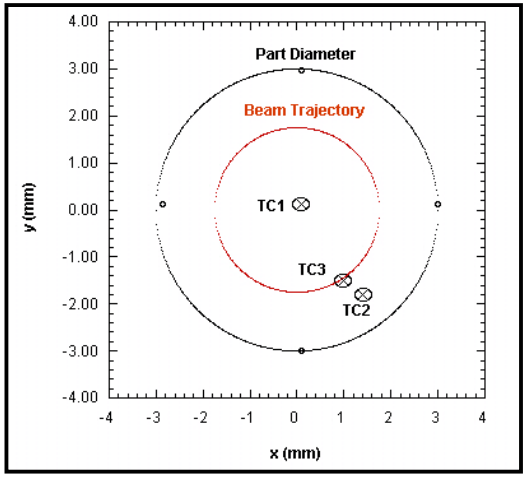

Thermocouple placement and beam trajectory relative positions.
TC1 is center-bottom; TC2 is edge-bottom and TC3 is edge-top.

Two types of samples:

- 304SS punched from shim stock
- 304SS annealed, chemically etched parts.

Discs measured 5.95 mm diameter by 0.127 mm thick, and averaged 0.0283g/disc

Sandia National Laboratories

Temperature Distributions and Gradient Changes in Laser Spin Forming

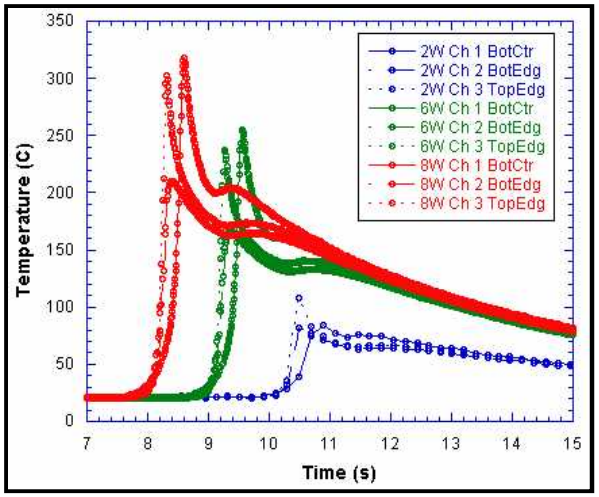

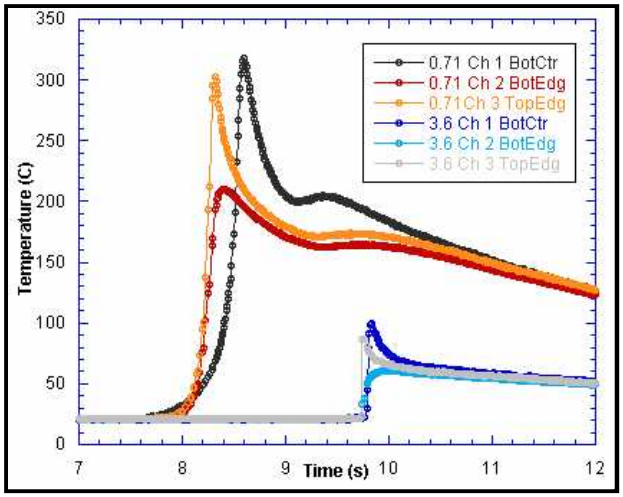

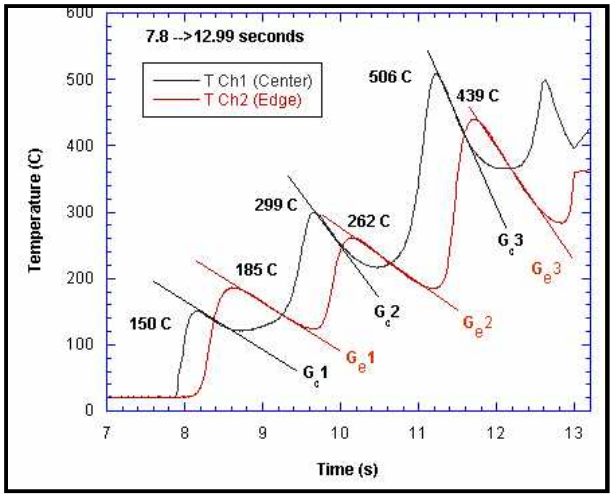

Etched 304SS disc
Variable laser power

- Three thermocouples
- 2, 6 & 8W
- 3.5 mm trajectory diameter
- 0.71 cm/s linear velocity (1 circuit)

Annealed 304SS disc
Variable scanner speed

Three thermocouples

- 8W
- 3.5 mm trajectory diameter
- 0.71 & 3.6 cm/s linear velocity (1 circuit)

Gradient shifting

- 8W
- linear speed ~ 0.71 cm/s
- Subset of multiple circuits

Sandia National Laboratories

Spin Forming Modeling: deformation

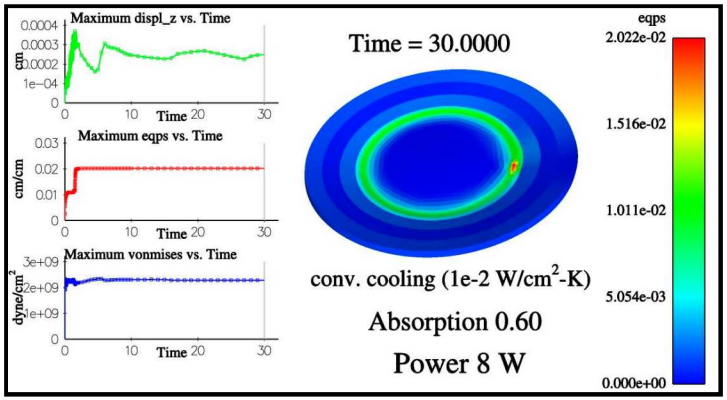

Equivalent Plastic strain predicted by Calagio FEM.

- For any permanent deflection to occur, the induced thermal strain must cause plastic deformation.
- The plastically strained region, represented by green area, is almost entirely limited to the same area the laser beam traversed.

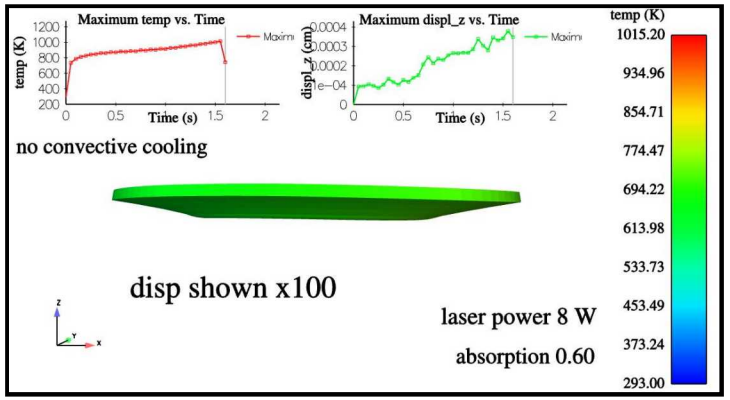

Calagio FEM displacement output.

- Total bend in displacement was predicted to be concave (towards the laser beam) on the order of 4mm after a single cycle.
- Experimental bend for the same conditions gave << 0.1mm total.

Sandia National Laboratories

Summary

- We've discussed distortion experiments and results for laser spot and seam welding of ~ 0.060" SS, and sub-melting laser spot bending of ~ 0.006" ***thin*** Au and SS materials.
- De-coupling the melting from the non-melting problem allows examination of transient, thermally induced strains and stresses and shows the increasing effects at smaller dimensions of TGM and BM distortions.
- Modeling inputs considering constrained vs. unrestrained motion, pre-existing residual stresses, thermal properties of the material, convective heat losses, geometry and processing conditions are increasingly important at smaller dimensions, and equally harder to determine.
- Analytic approaches can "loosen" some of the dependence on numerical approximations.
- Watanabe-Satoh treatment of laser seam welding was shown to correlate key relationships between controllable welding parameters (laser power, travel speed), weld size, and unrestrained angular distortion. Final distortion is considered to arise from two sources, the heat input (or temperature gradient) effect and the external restraint
- Transverse shrinkage was observed to be approximately linear with nQ/vt and increases monotonically with the width of the weld and a linear transformation of Watanabe's thermal factor mapped the angular distortion to weld size correlations.
- Laser bending (~20's mm deflection) of thin, high reflectivity, high conductivity, and high strength Neyoro-G™ strips and formed contacts was examined.
- At smaller dimensions, initial stress states and fixturing effects (restraint and thermal) have greater consequences

Future work

- Attempts will be made to recover the necessary parameters of the “thin” Au and SS parts to enable mapping those data points using the Watanabe-Satoh method and compare their correlations with more “macro” sized welds, to see if scale effects contribute significantly to the results.

- Additional temperature measurements will be made to further validate the computer model and aid in understanding the temperature gradients established in the thin sheet and their effects on TGM and BM regimes and transitions; especially as it relates to asymmetrical stress relief of existing residual stresses.

- Further study of the process parameter space response to the initial residual stresses state for < 0.010” parts will be undertaken. Additional study of heat extraction, cooling rates and further sample mounting ideas will be explored. A new 45W cw, 1091 nm fiber laser with a smaller, better quality raw beam (5.4mm diameter and M2 = 1.09) is now on-line and will be employed.

Acknowledgements

We would also like to thank:

J. Palmer, M. Kanouff, and J. Norris of Sandia National Laboratories and G. Roman University of Florida, Dept. Mech. Eng., Gainesville Fl,

Sandia National Laboratories